

The impact of the Early Cretaceous igneous intrusions in the Falkland Plateau Basin

Ana Filipa Dâmaso Duarte

filipadamasoduarte@gmail.com

Instituto Superior Técnico, Universidade de Lisboa, Portugal

October 2019

Abstract

The Falkland Plateau Basin is an sedimentary basin to the east of the Falkland Islands. The basin was created during the Gondwana breakup, on the Middle Jurassic, and was exposed to extensional forces during the South Atlantic Ocean opening. A system of magmatic intrusions are affecting the basin and date from the Early Cretaceous. The study of these features allows the comprehension of the basin formation as well as assess about the implication on the petroleum system.

Eight horizons were interpreted and there were identified 92 magmatic intrusions forming sills. All the surfaces were converted into depth using a velocity model based on literature. The geometries of the intrusions depend on the depth of emplacement. In greater depths, more planar tend to be the sills. The bottom sills are feeding the shallower sills due to the migration of material through the fractures. It is also possible to see two points where the magma extrudes, covering most part of the South-East area of the seismic volume.

Since these intrusions are contained in a package of black shale with a highly petroliferous potential dated from Upper Jurassic to Early Cretaceous, they could have contributed to the maturation of the source rocks in the basin. To infer about that possibility it was performed a Basin modelling study, by using a 1D basin model. The model was fitted to a set of pseudo-wells inside the seismic volume, in order to infer the maturation of the source rock for the entire area.

Keywords: Magmatic intrusions; Falkland Plateau basin; Sills; Seismic interpretation; Basin modelling.

1. Introduction

The magmatic events in the Falkland Plateau Basin are linked to tectonic processes. Its timing, extent and volume are a central piece of information to understand its implication in the sedimentary basin and in the petroleum system. The younger magmatic Cretaceous features on the Falklands Plateau basin are likely to have had a significant impact on the tectonic and thermal evolution of the basin, since the intrusions are emplaced in a series of shales with high petroliferous potential which could be a trigger to hydrocarbon generation, due to the possible effects on source-rock maturation. The work will focus on 3D mapping of sills and dykes, their geometry and spatial extent as well as their connection to extrusive features by an integrated interpretation of 2D and 3D seismic and exploratory well data. Finally, the thermal impact of the intrusions will be assessed by the

development of a basin model to test the maturity of the petroleum system.

2. Geological Setting

The Falkland Plateau Basin is located to the east of the Falkland Islands, in South America. This basin is part of a set of four submerged basins surrounding the Falkland Islands (Figure 1).

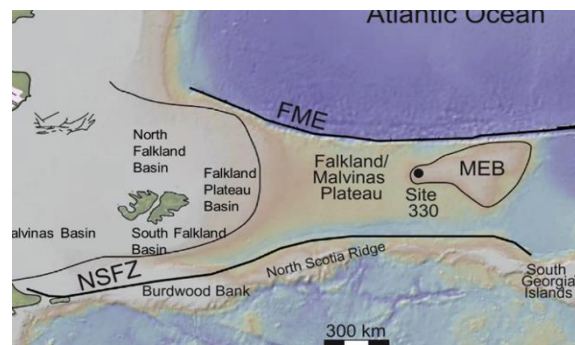


Figure 1 - Location of the Falkland Islands and surrounding basins. (modified from [2])

Before the Mesozoic Era (>~251 Ma), the Falkland Plateau was part of a supercontinent called Gondwana, then, during the Middle Jurassic (~170 Ma), the Antarctica plate started to drift from the mainland and the extensional forces created a large number of basins including the Falkland Islands Plateau basin [9]. This extensional movement promoted the development of NE-SW normal faults in the Falkland Plateau [18]. The second phase of extension occurred during the Early Cretaceous (~140 Ma), when Falkland Plateau basin was exposed to other extensional forces coming from the opening of the South Atlantic ocean [8].

The sedimentary succession was affected by an extensive series of intrusive magmatic dykes and sills, and extrusive volcanic lavas. There are two different types of dykes exposed on the Falkland Islands, from two different geological times [22]. The first intrusive event occurred during the Jurassic (~178Ma), and it is probably related to the magmatic intrusions in the Karroo Basin [20]. The second system of magmatic intrusions is dated from the Cretaceous, from 121.3 ± 1.2 Ma [22] to $133-138 \pm 4$ Ma [20] and have an N-S trend. These dykes were discovered by [1] but its age was inferred later [22]. These intrusions were formed during the South Atlantic Ocean and North Falkland Basin opening [22]. The dykes have the same trend as the faults seen on the North Falkland Basin and its emplacement could have been linked with the stress regime felt in that area [22].

The lavas seen on the Falkland Plateau basin by [16], have relative dating from the Valanginian – Hauterivian, the same age for the Early Cretaceous dykes reported by this author. These magmatic rocks are well studied onshore but the link between the offshore expressions are still poorly understood.

The DSDP core acquisitions from Site 330 and Site 511 allowed to extract information about the different lithologies present in the stratigraphic column from Middle Jurassic to Present.

From Late Jurassic to Aptian were found black shales with high petroliferous potential with a TOC ranging between 3-8% [3]. The same unit was found in new drilled wells as a succession of black shales interbedded with sandstones with reservoir qualities, prevent from turbiditic fans [5].

2.1 Petroleum System

In the Falkland Plateau Basin at least three wells were drilled, TOROA, Humpback and Loligo-A. TOROA was characterized as a dry well. However, Humpback had gas shows but not in commercial amounts. Loligo-A in another way possibly has large amounts of gas in place and poor quality reservoirs [24].

2.1.1 Source-rock: The main source rocks in the basin are black shales from Early Cretaceous, evidence from DSDP well reports and from TOROA well reports. From TOROA well report we have the information that the hydrocarbons are from Type II and III (oil/gas prone), the maturity was not reached in this location and the TOC percentage ranges from 0,56 to 18,4%. TOC percentage above 4% indicates very good source rock with high petroleum potential [12].

2.1.2 Reservoir rocks: The sandstones that are interbedding with the black shales (seen on TOROA well) and by [5] are the principal reservoir rocks. Siltstones and Limestones from Late Cretaceous (seen on DSDP wells) can also work as reservoir.

2.1.3 Seal rocks: Known as regional seal are the Claystones from the Aptian [6]. Clay-rich Diatomites from the beginning of Paleogene can also have seal properties due to its high content in clay.

2.1.4 Traps: To the NW part of the basin, there are some deepwater sand fans that can act as trap to hydrocarbons [6]. The clinofolds succession with pinch-out layers can also trap hydrocarbons due to its structure.

3. Seismic reflection data interpretation

Seismic reflection data provide an approximated image of the subsurface. Usually, the data is visualised as vertical cross-sections that allow seeing geologic structures of the subsurface. The interpretation performed using cross-sections in two way travel time (TWT) for the vertical axis and in meters for the horizontal axis. For the 2D data lines, the interpretation was made throughout some of the lines that have more importance for the objectives of this work.

The interpretation of the 3D seismic volume followed a grid of inlines and crosslines with an established distance between each. This helps the accurate interpretation of structures with high spatial variability, which can help the interpretation of complex geologic

structures. For less complex structures a 3D auto-track can be used directly in a more expedite way of interpretation.

3.1 Horizon interpretation

In this project the interpretation of surfaces is important to correctly assess the burial history of the region as well as to enclosure the magmatic event in time and space. The interpretation of horizons was performed by looking for the seismic sequences, identifying the geometry of reflections terminations and discontinuities. From that interpretation resulted eight horizons corresponding to a thick sedimentary succession from the Jurassic rifting phase (S5) until the present Sea bottom.

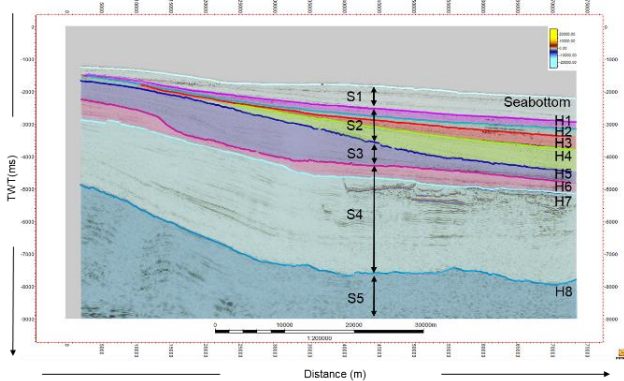


Figure 2 - Interpreted inline and the corresponding sequences. Horizons as H1 to H8 and sequences as S1 to S5.

By mapping the surfaces it is visible a trend of subsidence from East to West, highlighting the transition between a shelf and a deep marine environment.

Sequence 4 is the most important sequence for this work, it is delimited on the bottom by horizon 8, which corresponds to the top of the Jurassic rifting phase, and on top by the top of Aptian. This succession is highly intruded by the Cretaceous magmatic bodies and according to the literature there is where a succession of source-rocks are present [5].

3.2 Fault planes

Considering exclusively the 3D seismic data, the interpretation of faults was done by interpreting diverse horizontal time slices from the seismic cube. To help the visualization of the fault planes, seismic attribute analysis was used to highlight discontinuities. The variance attribute was computed over the original amplitude volume. This seismic attribute measures the similarity in waveform and lateral change of the reflector amplitude for adjacent traces [16].

According to the observations and correlating the analysis with the literature [5], the 3D FISA volume presents almost no faulting, not being distinguished any regional fault or rift geometries.

By interpreting the Variance seismic volume, it is attainable to interpret some fracture planes inside the desired sequence (S4) between H7 and H8.

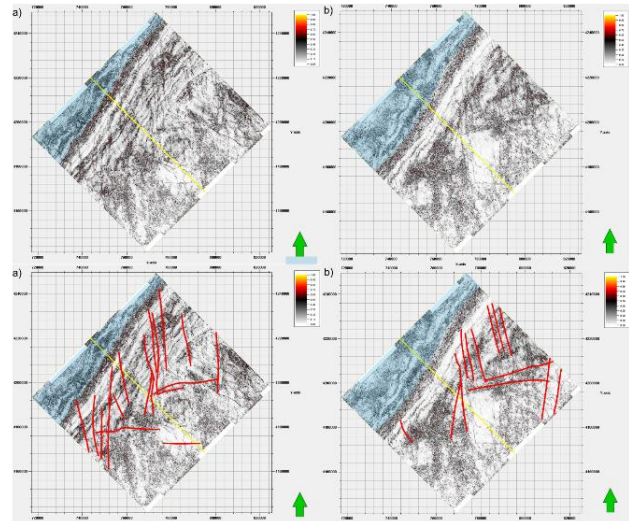


Figure 3 - Time slices of the Variance attribute cube. A) corresponds to time slice -5600ms. B) corresponds to time slice -6200ms. (H8 in blue).

From Figure 3, we obtain two main directions of faulting, mainly oriented from NNW to SSE and a second direction from WSW to ENE. Being these prolonged vertically through the sequence.

3.3 Magmatic Intrusions

Igneous intrusions can have seismic signatures such as in Figure 4.

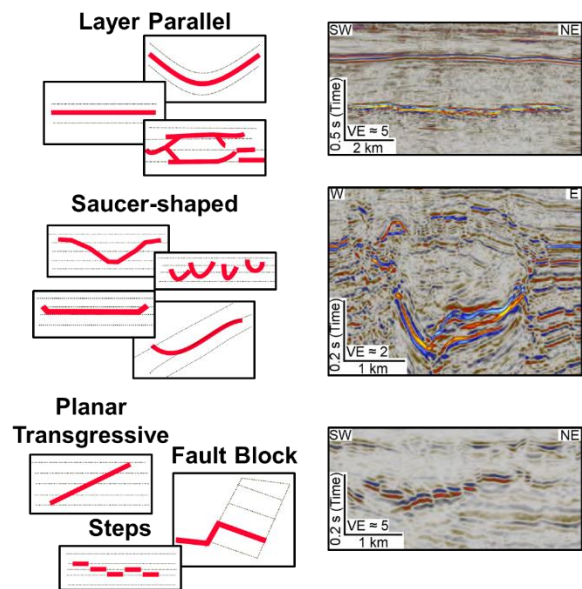


Figure 4 - Seismic signatures (re-drawn from [17] and [11]).

Sill migration generally starts with the formation of a deeper sill, circular in shape, the feeding point of this sill usually is near the centre of the circle. The magma follows with a planar geometry in the centre part, until the tips of the sill start to follow a more transgressive flow path [13]. The deeper sill tips serve as a feeding point for shallower sills. Shallower sills tend to be more saucer-shaped as the deeper ones, this is due to the stress field created by the overburden rocks. It's possible to say that the diameter of intrusions is dependent on the depth of emplacement, increasing with depth (Figure 5) [7].

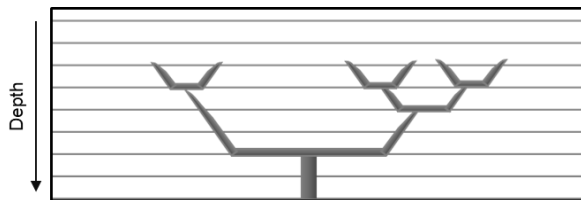


Figure 5 - Schematic representation of the sill emplacement depending on the depth.

The emplacement of intrusions in shallower layers leads to uplift and folding of overlying strata, this jack-up will allow inferring the relative intrusion timing. [10].

The intrusions were interpreted in the 3D volume individually. The interpretation was done by following the sill reflections going from inline to inline and crossline to crossline in a short grid since the lateral extension of each sill is different and variable in space. The vertical intrusions, denominated as dykes, are difficult to see, but they can cause some amplitude anomalies and discontinuities, and be identified because of that.

A top and a bottom reflection were interpreted for each sill. The top reflection is a hard event (colour red in this seismic) due to increase in impedance, the bottom reflection is a soft event due to decrease of impedance (colour blue in this seismic) (Figure 6). The top and bottom reflections translate the top and base of the sill itself.

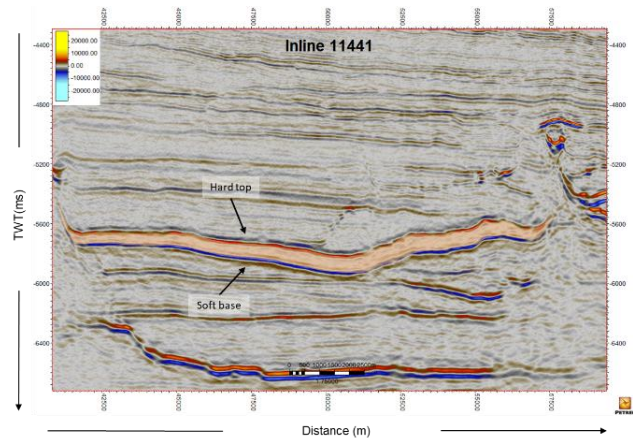


Figure 6 - Representation of a sill on seismic, showing the top and base reflections.

All the intrusions analysed during this thesis are found on the SE part of the 3D volume. They are spread to a total of 4991,6 km² and they are occupying a volume around 260 km³. The average thickness doesn't overtake the 220 m.

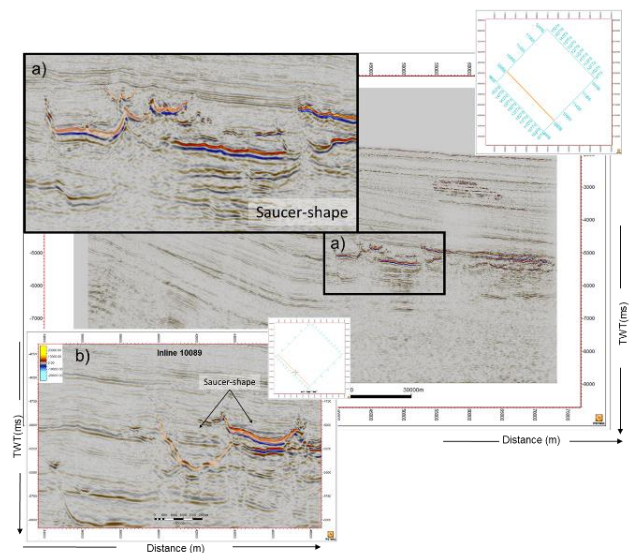


Figure 7 - Saucer-shaped geometries of intrusions

The main sills geometries fall in the saucer-shaped category (Figure 7), although there are other expressions, less common through the volume, that resembles stepping (Figure 8).

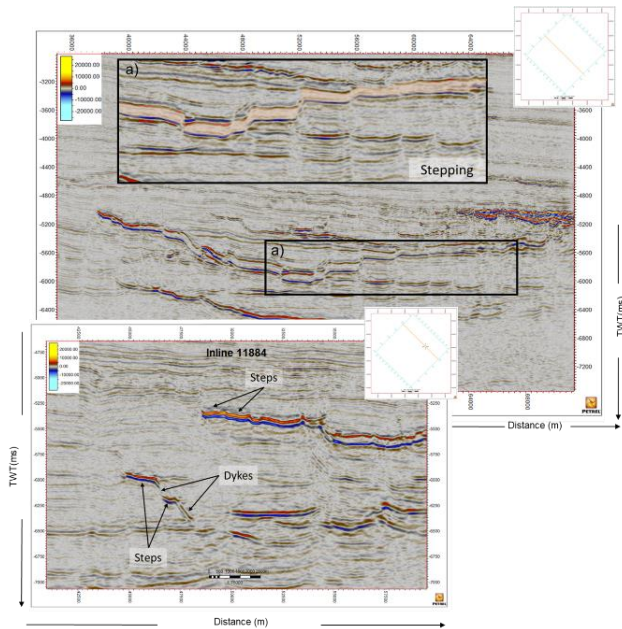


Figure 8 - Intrusions emplaced as steps. Dykes serving as magma migration pathways.

During this study, a large and central sill in the deepest portion of Unit 8 was interpreted. This sill is believed to be the one that influences the magma propagation. It has an inner centre with a planar expression followed by transgressive tips, which are ending on shallower sills (Figure 9).

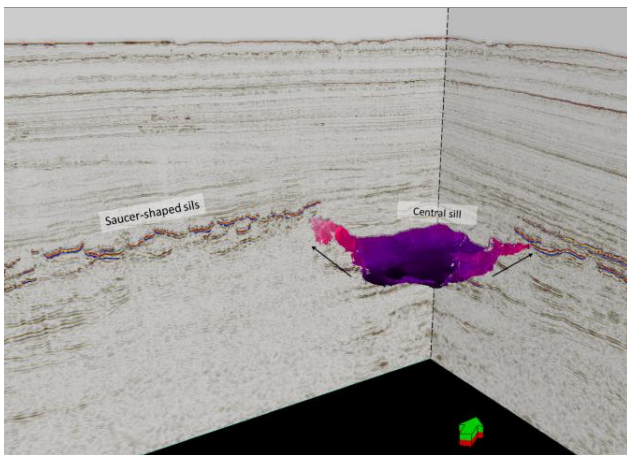


Figure 9 - Central sill feeding shallower sills.

Some sills are being fed by transgressive ends of the deeper ones and others are filled through dykes. The magma is exploiting fractures to get to the upper layers, the dyke material is filling them.

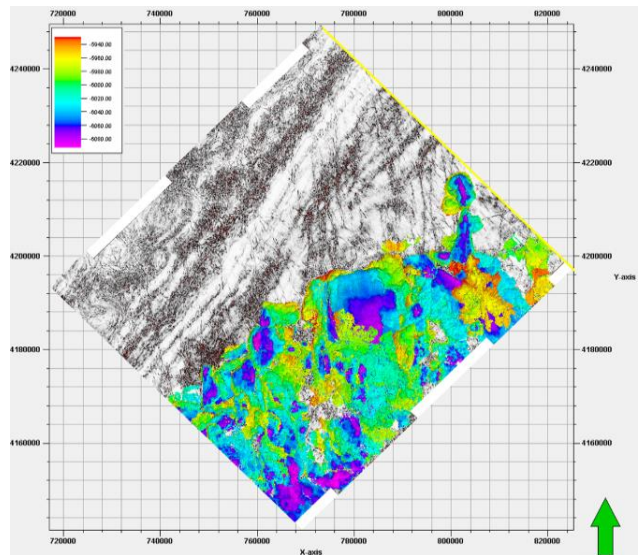


Figure 10 - Map of intrusions plotted on top of a Variance attribute time slice.

Figure 10 shows a map view with all the interpreted intrusions. When plotted on top of the fractures map it is evident a correlation between the sills orientation and the fracture planes. The sills are oriented in two directions from: NW to SE and from WSW and ENE. The first direction is likely the main direction of propagation, the sills inner part (deepest one) are corresponding to this direction, however the second direction looks like some barrier for propagation, the sills borders are terminating against this direction.

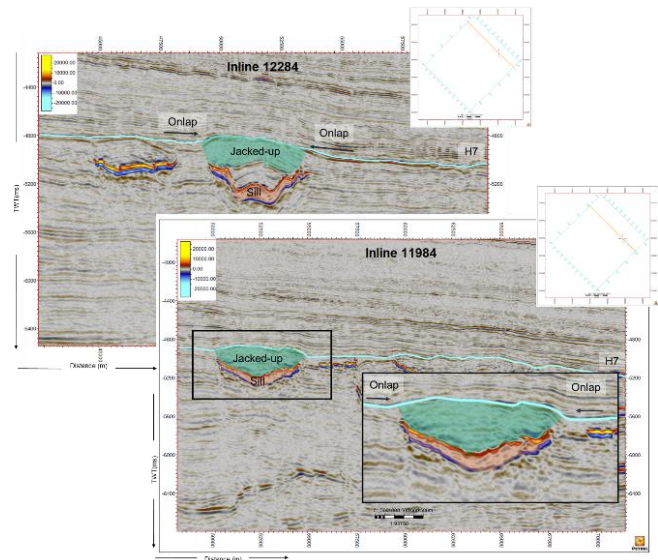


Figure 11 – Layer H7 that is jacked-up and onlap details.

In Figure 11 it is visible that the intrusions are jacking-up layer H7, new layers are onlapping H7. This means that the magmatic intrusions are younger than the strata below H7 but older than the layers overlying H7.

Accordingly with literature ([19] and [5]) this horizon 7 is dated from the Valanginian age, being possible to say that the intrusions are dating from this time.

3.4 Lavas

Lava flows have different morphologies conditional on its eruption environment as seen by [17]. As the intrusions, lava extrusions are also related to high seismic amplitudes, due to volcanic units with high impedance. The principal point for studying the lavas in this project is to assess its extent within the area of interest. In this basin, the lavas are present as sheet flow and therefore only the top layer was interpreted due to difficulties of distinguishing reflections from its base. The internal facies show chaotic texture as also some parts of subparallel characteristics. The eruption point for the lavas was also analysed. Some extruded material is present on the SE part of the volume being found on top of the intrusions.

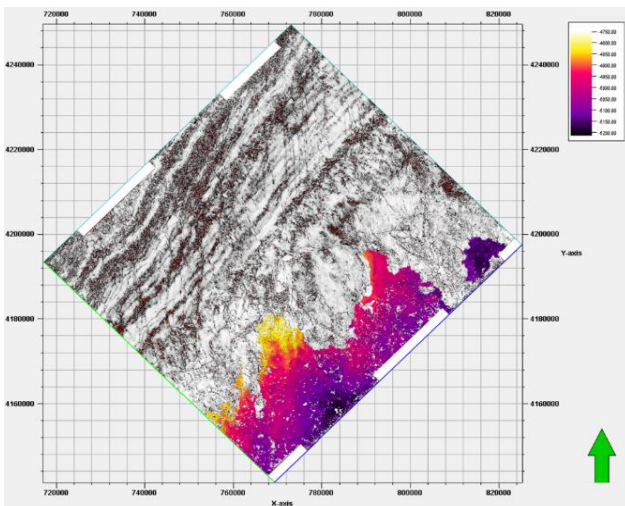


Figure 12 - Interpretation of the lavas top in map view – Variance attribute time slice.

The extrusions are likely to have been fed in two points where the intrusions got to shallow allowing the magmatic material to flow on the surface.

3.5 Escape features

Knowing, from the geological setting of the Falkland Plateau Basin, that the intrusions are affecting rocks with high petroliferous potential it is expected to find fluid escaping structures, being the fluids water, gas or even oil. In the seismic data, there are some interesting features, such as bright reflections, on the upper layers of the stratigraphy resemble fluid accumulation, that might be direct hydrocarbon indicators. These bright

spots are highly connected with the intrusions, especially the Central Sill (Figure 13).

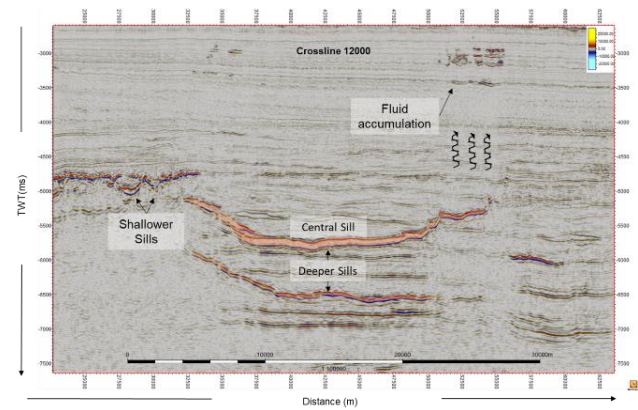


Figure 13 - Fluid accumulation on top of the tips of the Central Sill.

4. Seismic reflection interpretation discussion

After an in-depth study of the observations is feasible to make some considerations:

- The stratigraphic layers are subsiding from West to East, probably going this way until the basin depocenter.
- The intrusions are dating from Early Cretaceous, Valanginian – Barremian age and are bounded by horizon 7 and 8.
- The intrusions show mainly saucer-shaped geometries and corroborates the theory of [7].
- The Central Sill has a planar with transgressive ends geometry and feeds shallower sills through the fractures, having the shallow ones a more evident saucer-shaped geometry.
- More shallow the sills are, more saucer-shaped they appear and with decreased area.
- The intrusions are aligned with the fault planes, being these the principal pathway for magma migration. The magma is thus intruding and exploiting faults to get to upper levels of stratigraphy.
- In two points, the magmatic material gets to shallow that extrudes, creating a lava layer. The seismic characteristic of the extrusions indicates a subaqueous flow, a paleo water depth of <100 during that time.
- The lavas are overlaying the surface H7 what indicates that they are contemporaneous with the magmatic intrusions.
- On top of the intrusions, it is found an accumulation of fluids in the upper layers, this can be due to intrusion of magma in high petroliferous layers. The heat can have impacted the maturation and expulsion of hydrocarbons.

5. Basin Modelling

In order to understand the maturity of the source-rocks and its spatial distribution inside the basin, this chapter introduces a study for the assessment of the thermal maturity of the source-rock, subsidence and expulsion of hydrocarbons for the Falkland Plateau Basin. Previous basin modelling works, done in the basin, predicted temperature too low, reviling a cooler basin compared with new insights from Humpback and Loligo-A wells [4].

PetroMod® was used for the basin modelling and applied to 1D models, created within the seismic inversion grid. The resulting 1D models were then used to estimate the thermal maturation for the entire region of interest using geostatistical simulation. Basin modelling consists in a backstripping simulation which comprises the recreation in time and vertically in space of the deposition and subsidence history of the basin, and evaluating how these processes affect the temperature and the organic matter maturation of the source-rocks as well as its hydrocarbon generation potential and spatial distribution [23].

5.1 Basin modelling methodology

The next figure (Figure 14) is a schematic representation of the workflow done on the 1D basin modelling.

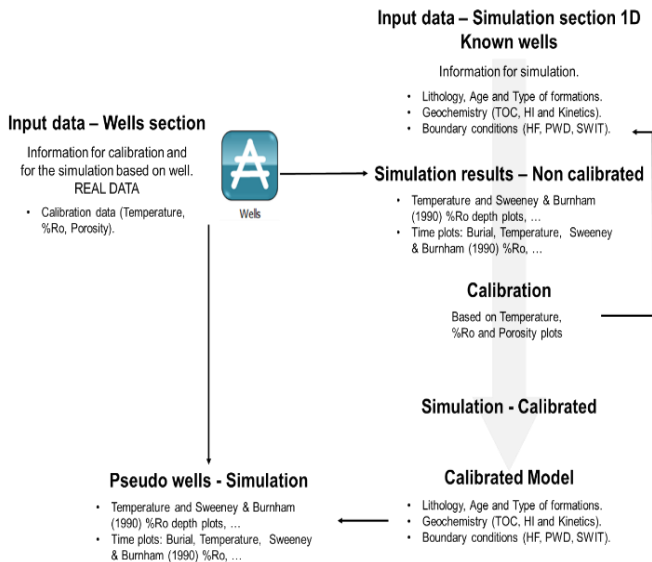


Figure 14 - Schematic representation of the workflow for the basin modelling

5.2 Basin modelling input

As the study area corresponds to an underexplored basin, during literature review very little information was found regarding the wells near the seismic volume, only

information from TOROA was provided. And was also used the information and data from Deep Sea Drilling Project, DSDP wells 511 and 330 drilled in the basin. This data were crucial to perform and calibrate the basin modelling. The core data of DSDP wells were found online on Scientific Earth Drilling Information Service - SEDIS. Data from TOROA were taken from well reports.

5.2.1 Stratigraphy: The following figure (Figure 15) represents the stratigraphy of each drilled well and pseudo-wells.

	DSDP 330	DSDP 511	TOROA	Seismic Interpretation	Pseudo-wells	Petroleum System Elements
QUATERNARY		SANDY GRAVEL	SANDY GRAVEL			
PLIOCENE		DIATOM OOZE				
MIOCENE				Unit 1	Sandstone	Overburden rock
OLIGOCENE						
Eocene		DIATOMACEOUS OOZE & CARBONATE				
PALAEOCENE					Diatomite	Seal Rock
MAASTRICHTIAN				Unit 2	Claystone	Seal Rock
CAMPANIAN		ZEOLITIC CLAYSTONE				
SANTONIAN				Unit 3	Limestone	Reservoir
TURONIAN				Unit 4	Siltstone	Reservoir
CENOMANIAN						
ALBIAN		NANNO CLAYSTONES (OPEN OCEAN)	CLAYSTONE (HIGH PETROLIFEROUS POTENTIAL)	Unit 5	Claystone	Seal Rock
APTIAN						
BARREMIAN				Unit 6		
HAUTERVIAN						
VALANGIAN					SANDSTONE & BLACK SHALES SUCCESSION	Reservoir rocks interbedded with source-rocks
BERRIASIAN						
TITHONIAN				Unit 7		
KIMMERIDGIAN						
OXFORDIAN						
CALLOVIAN						
BATHONIAN				Unit 8	Claystone	Underburden rock
BAJOCIAN						
PRE-CAMBRIAN/EARLY PALAEOZOIC		GRANIT & GNEISS				

Figure 15 - Stratigraphy correlation between wells and seismic interpretation.

The geochemical parameters to be imposed to the generator units correspond to the Hydrogen Index (HI), Total Organic Carbon (TOC) and Kinetic model. For the calibration wells it is easy to acquire HI and TOC values from the geochemistry test done to the wells, present on well reports.

The Kinetic models used were the ones built by [15]. These models are often indicated to projects where there is no geochemical information and where the uncertainty is high.

5.2.2 Calibration data and boundary conditions: The data (Table 1) from the known wells (TOROA, DSDP 511 and DSDP 330) was introduced in the well section as calibration data.

Table 1 - Input data.

	Site 511	Site 330	TOROA
Temperature	<input checked="" type="checkbox"/> Calculated	<input checked="" type="checkbox"/> Calculated	<input checked="" type="checkbox"/> From well data
HI	<input checked="" type="checkbox"/> From well data	<input checked="" type="checkbox"/> no data	<input checked="" type="checkbox"/> From well data
Vertical Thermal Conductivity	<input checked="" type="checkbox"/> From well data	<input checked="" type="checkbox"/> no data	<input checked="" type="checkbox"/> no data
Tmax	<input checked="" type="checkbox"/> From well data	<input checked="" type="checkbox"/> no data	<input checked="" type="checkbox"/> From well data
%TOC	<input checked="" type="checkbox"/> From well data	<input checked="" type="checkbox"/> From well data	<input checked="" type="checkbox"/> From well data
%Ro	<input checked="" type="checkbox"/> From well data	<input checked="" type="checkbox"/> no data	<input checked="" type="checkbox"/> Calculated
Porosity	<input checked="" type="checkbox"/> no data	<input checked="" type="checkbox"/> From well data	<input checked="" type="checkbox"/> no data

The paleowater depth (PDW) was inferred using the lithology and the probable deposition environment, as well as by analysing the type of microorganisms present in the samples (from well reports). On TOROA well, the biostratigraphy report has a description of the paleowater environment for deposition, only needing a numeric attribution of the metric depth.

For the Surface-Water Interface Temperature (SWIT), the input parameters are equal for each well (South Hemisphere, South America), only changing the Latitude. After giving that information the software generated the table for SWIT. Although, these values were changed to match the present day temperature. This temperature was assumed to be 2°C [14]. After running the simulation, a set of results were studied and adjusted. The adjustment of the simulated curve with the real values was done by changing the Heat Flow values (Figure 16) being this the biggest variable that affects the model. It was needed to find a commitment between the simulated curves for each well.

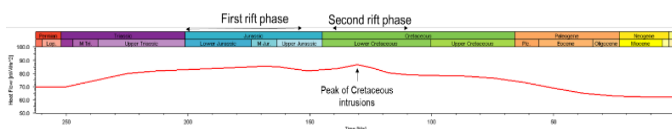


Figure 16 - Best model interpretation for the Heat Flow for site 511, 330 and TOROA.

5.2.3 Pseudo-wells: After model calibration a grid of pseudo-wells within the seismic volume was created (Figure 17). This approach allows the study of the maturation of the source-rock inside the volume, where the seismic interpretation was done. The grid was created using an equal distance between pseudo-wells, a radius of 15km. By having a grid of 25 pseudo-wells in total it is possible to study the maturation inside the volume by predicting the spatial distribution of the simulated values.

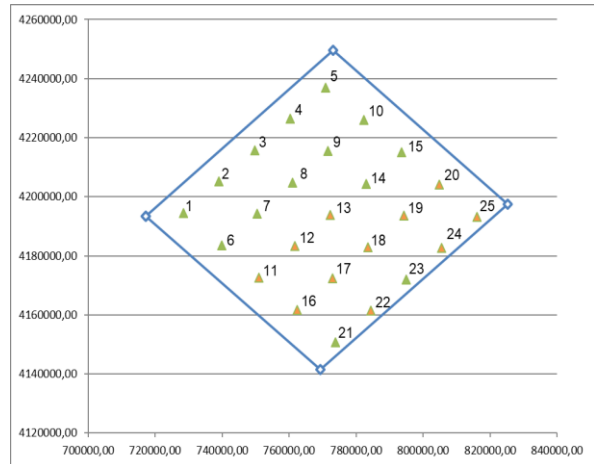


Figure 17 - Grid of pseudo-wells inside FISA boundaries, in orange the pseudo-wells that are intersecting sills.

After run each model from each pseudo-well, the maturation data from the source rocks (Sequence 4) were used as input to a Sequential Gaussian Simulation (SGS) using a model grid of 1000x1000x50m. A variogram was adjusted to the values. After run the simulation it was obtained 100 simulation cubes with equal possibility of occurrence.

The resulting maturation cubes correspond to continuous values of Vitrinite Reflectance (%Ro). The 100 maturation cubes were then used to compute the probability of a single maturation class to happen through the grid. The probability volume allows to assess the most probable maturation at each location within the area of interest.

5.3 Basin modelling results:

The simulated values of temperature through each pseudo well are reproducing fairly the Geothermal gradient known for the basin [14]. The %Ro values through the pseudo-wells are increasing with depth. The maturation of the source-rocks from the pseudo-wells show greater maturation when comparing to the ones on the known sites. This is a normal occurrence since the stratigraphic layers of the pseudo-wells are buried deeper than the ones in the known wells, which is translated in exposure to higher temperatures. An increasing in maturation is also visible from pseudo-well to pseudo-well depending on the depth of burial of the source rock from point to point. When magmatic intrusions are present in the well it is clear an abrupt increase of %Ro which can be translated in overmaturation.

The one hundred realization were classified in terms of Valanginian are shown on Figure 18 and Figure 19, maturation and had the probability of each class respectively. computed. The probabilities for layer Aptian and

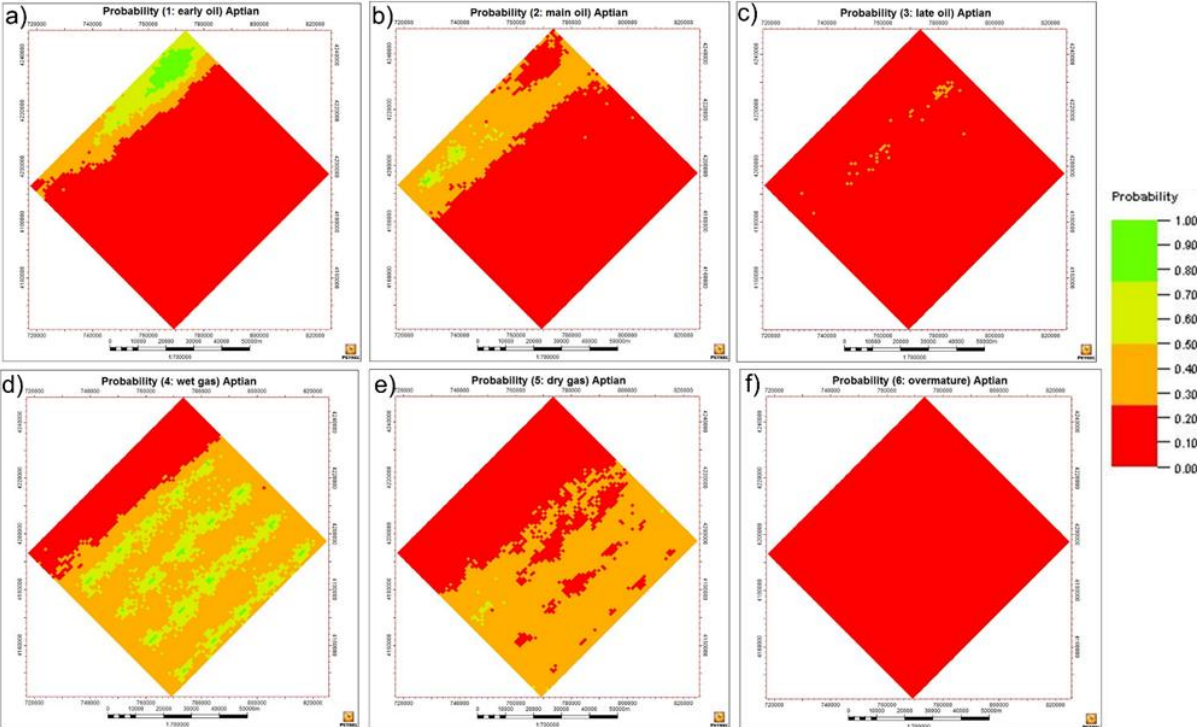


Figure 18 - Probability of each category in the Aptian surface.

From the maps of Aptian (Figure 18) it is possible to dispersed prominence of Wet gas to the SSE. see a prominence of Early oil to the NNW and a

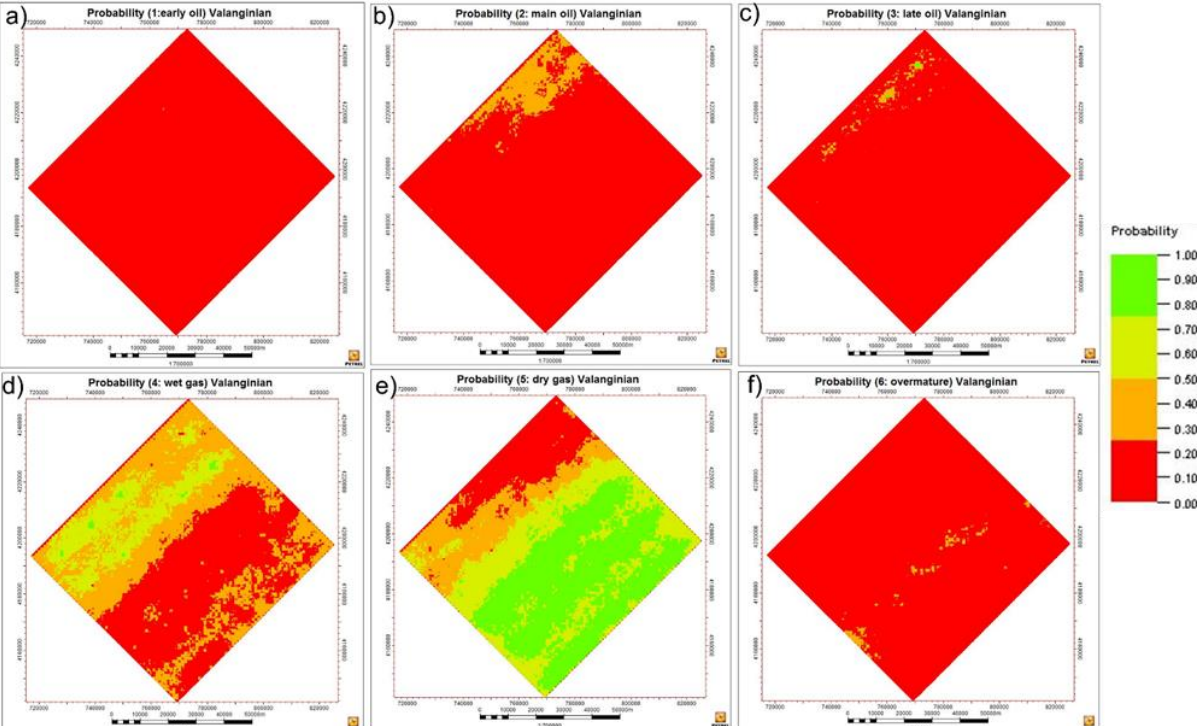


Figure 19 - Probability of each category in the Valanginian surface.

From the maps of Valanginian (Figure 19) it is possible to see a prominence of Wet gas to the NNW and a dispersed prominence of Dry gas to the SSE, being this category the most probable for these layers.

6. Basin modelling discussion

Accordingly to the model, it is notorious an overmaturation of most of the volume (Figure 20) in

layers older than the Valanginian. Although in the shallower parts (younger than Valanginian) to the NNW there are still oil from the first and second stage. Dry Gas is the second category most probable to be found to the SSE of the volume, shallower in that part is probable to find Wet Gas.

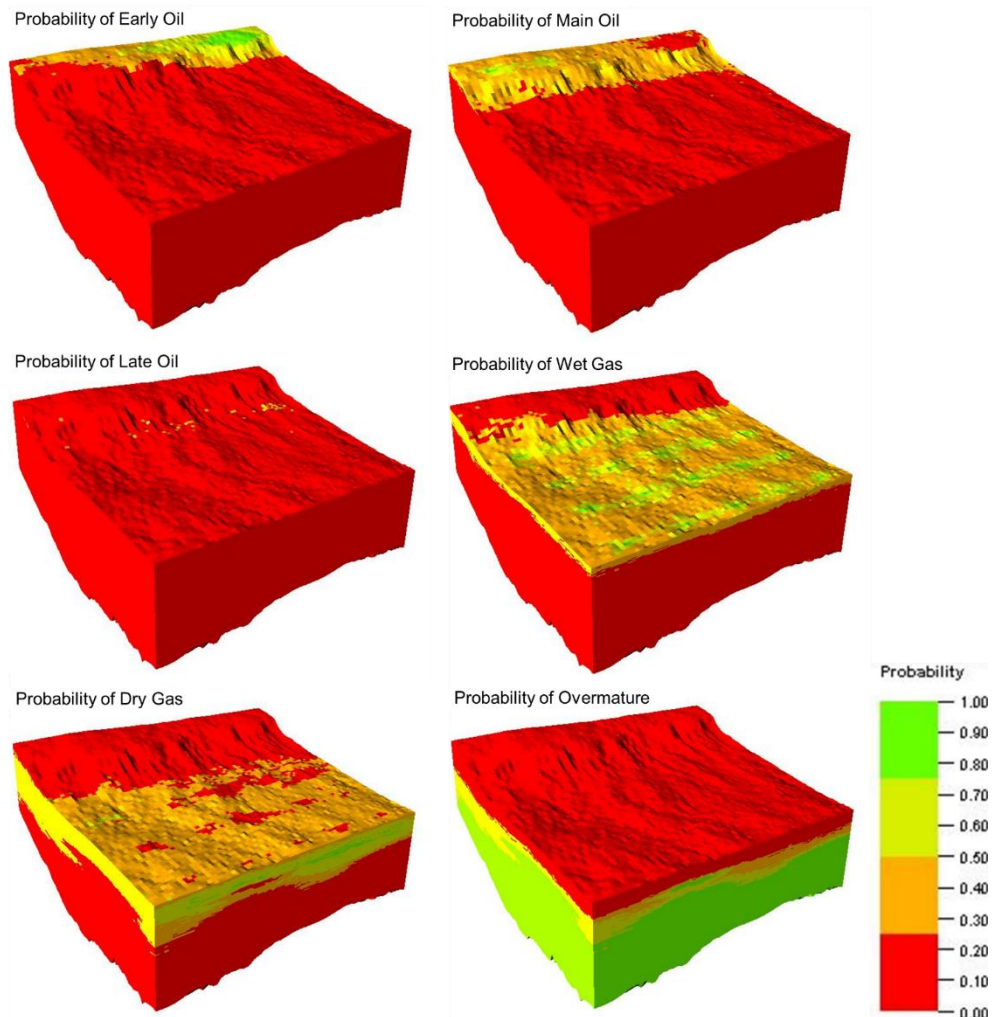


Figure 20 - Probability cubes for the model with magmatic intrusions.

7. Final considerations

The intrusions present on the basin are gathered to the SSE of the interpreted volume. They are probably dispersed and also present beyond the interpreted volume (observed on the 2D lines).

It is evident an Overmaturation of the deepest source-rocks. It is more probable to find Wet gas (to the NNW) and Dry gas (to the SSE) near the Valanginian layer, and the first stages of oil (to the NNW) and Wet gas (to the SSE) near the Aptian layer.

8. References

- [1]Barker, P.F.. 1999. Evidence for a volcanic rifted margin and oceanic crustal structure for the Falkland Plateau Basin. *Journal of the Geological Society*,156(5):889. doi:10.1144/gsjgs.156.5.0889
- [2]Chemale, F., Ramos, V., Naipauer, M., Girelli, T., Vargas, M.. 2018. Age of basement rocks from the Maurice Ewing Bank and the Falkland/Malvinas Plateau. *Precambrian Research*, vol. 314. doi:10.1016/j.precamres.2018.05.026
- [3]Deroo, G., Herbin, J., Roucaché, J.. 1983, Organic geochemistry of upper Jurassic-Cretaceous sediments at DSDP Hole 71-511, PANGAEA. doi:10.1594/PANGAEA.815172
- [4]Fratlicelli, C., Yusri, Y., Mercer, J., Yezerski, D., Stearman, M.. 2017. Evidence of Cretaceous Plate Collisions along the Falkland Plateau Basin - Ramifications for Petroleum Systems and Reservoir Quality. Poster - 2017 AAPG Annual Meeting.
- [5]Fratlicelli, C., Yusri, Y., Miller, S., Salamoff, S., Yezerski, D., Mercer, J., Reece, J., Bova, J., Gomez, J.. 2016. Linked Shelf to Deepwater Systems in the Southern Falkland Plateau Basin – Controlling Mechanisms, Stratigraphic Packaging, and Petroleum Potential. Conference paper - AAPG Annual Meeting 2016.
- [6]Fratlicelli, C..2016. Rift Basin Characteristics Derived from Antecedent Tectonic Events – Intricacies of the Falkland Plateau. Conference: AAPG 2016, At Calgary, Alberta, Canada
- [7]Galland, O., Planke, S., Neumann, E., Malthé-Sørenssen, A., 2009. Experimental modelling of shallow magma emplacement: Application to saucer-shaped intrusions, *Earth and Planetary Science Letters*, Volume 277, Issues 3–4, doi:10.1016/j.epsl.2008.11.003.
- [8]Hall, S., Bird, D., McLean, D., Towle, P., Grant, J., Danque, H.. 2018. New constraints on the age of the opening of the South Atlantic basin. *Marine and Petroleum Geology*, Volume 95. doi:10.1016/j.marpetgeo.2018.03.010
- [9]MacDonald, D., Gomez-Perez, I., Franzese, J., Spalletti, L., Lawver, L., Gahagan, L., Paton, D.. 2003. Mesozoic break-up of SW Gondwana: implications for regional hydrocarbon potential of the southern South Atlantic. Volume 20, Issues 3–4, doi:10.1016/S0264-8172(03)00045-X
- [10]Magee, C., Jackson, C., Hardman, J., Reeve, M.. 2017. Decoding sill emplacement and forced fold growth in the Exmouth Sub-basin, offshore northwest Australia: Implications for hydrocarbon exploration. *Interpretation*, Volume 5, Issue 3. doi:10.1190/INT-2016-0133.1
- [11]Magee, C., Maharaj, S., Wrona, T., Jackson, C.. 2015. Controls on the expression of igneous intrusions in seismic reflection data. *Geosphere*, 11 (4) doi:10.1130/GES01150.1
- [12]Magoon, L. B. and Dow, W. G.. 1994. *The Petroleum system: From source to trap*. Tulsa, Oklahoma. AAPG memoir, 60. ISBN: 0891813381.
- [13]Malthé-Sørenssen, A., Planke, S., Svensen, H., Jamtveit, B., 2004. Formation of saucer-shaped sills. *Geological Society London Special Publications*. 234. 233-241. doi:10.1144/GSL.SP.2004.234.01.13.
- [14]Nicholson, U. and Stow, D., 2019. Erosion and deposition beneath the Subantarctic Front since the Early Oligocene, *Scientific Reports*, 9, 1, 2045-2322. doi:10.1038/s41598-019-45815-7
- [15]Pepper, A.S., Corvi, P.J., 1995 Simple kinetic models of petroleum formation. Part I: oil and gas generation from kerogen, *Marine and Petroleum Geology*, Volume 12, Issue 3, 291-319. [https://doi.org/10.1016/0264-8172\(95\)98381-E](https://doi.org/10.1016/0264-8172(95)98381-E)
- [16]Pereira, L.. 2009. *Seismic Attributes in Hydrocarbon Reservoirs Characterization*. Master's thesis, Departamento de Geociências, Universidade de Aveiro.
- [17]Planke, S., Alvestad, E., Eldholm, O.. 1999. Seismic characteristics of basalt extrusive and intrusive rocks. *The Leading Edge*. 18. 342-348. doi:10.1190/1.1438289
- [18]Planke, S., Rasmussen, T., Rey, S., Myklebust, R.. 2005. Seismic characteristics and distribution of volcanic intrusions and hydrothermal vent complexes in the Vøring and Møre basins. *Geological Society, London, Petroleum Geology Conference series*, 6, 833-844. doi:10.1144/0060833
- [19]Richards, P., Gatliff, R., Quinn, M., Fannin, N., Williamson, J.. 1996. The geological evolution of the Falkland Islands continental shelf. *Geological Society, London, Special Publications*, 108. doi:10.1144/GSL.SP.1996.108.01.08
- [20]Richards, P., Stone, P., Kimbell, G., McIntosh, W., Phillips, E.. 2013. Mesozoic Magmatism in the Falkland Islands (South Atlantic) and their offshore sedimentary basins. *Journal of Petroleum Geology*, Volume36, Issue1. doi:10.1111/jpg.12542
- [21]Schimschal, C., Jokat, W.. 2018. The crustal structure of the continental margin east of the Falkland Islands. *Tectonophysics*, Volume 724. doi:10.1016/j.tecto.2017.11.034
- [22]Stone, P., Richards, P., Kimbell, G., Esser, R., Reeves, D. 2008. Cretaceous dykes discovered in the Falkland Islands: implications for regional tectonics. *Journal of the Geological Society*, 165 (1) doi:10.1144/0016-76492007-072
- [23]https://wiki.aapg.org/Basin_modeling:_identifying_and_quantifying_significant_uncertainties – seen on 14th of October of 2019
- [24]<https://www.fig.gov.fk/minerals/> – seen on 27th of August of 2019